MULTI-BODY ANALYSIS OF THE 1/5 SCALE WIND TUNNEL MODEL OF THE V-22 TILTROTOR

G. L. Ghiringhelli P. Masarati[1] P. Mantegazza

Politecnico di Milano
Dipartimento di Ingegneria Aerospaziale
Milano, Italy

M. W. Nixon

Army Research Laboratory
NASA Langley Research Center
Hampton, VA 23681

Abstract

The paper presents a multi-body analysis of the 1/5 scale wind tunnel model of the V–22 tiltrotor, the Wing and Rotor Aeroelastic Testing System (WRATS), currently tested at NASA Langley Research Center. An original multi-body formulation has been developed at the *Dipartimento di Ingegneria Aerospaziale* of the *Politecnico di Milano*, Italy. It is based on the direct writing of the equilibrium equations of independent rigid bodies, connected by kinematic constraints that result in the addition of algebraic constraint equations, and by dynamic constraints, that directly contribute to the equilibrium equations. The formulation has been extended to the simultaneous solution of interdisciplinary problems by modeling electric and hydraulic networks, for aeroservoelastic problems. The code has been tailored to the modeling of rotorcrafts while preserving a complete generality. A family of aerodynamic elements has been introduced to model high aspect aerodynamic surfaces, based on the strip theory, with quasi-steady aerodynamic coefficients, compressibility, post-stall interpolation of experimental data, dynamic stall modeling, and radial flow drag. Different models for the induced velocity of the rotor can be used, from uniform velocity to dynamic inflow. A complete dynamic and aeroelastic analysis of the model of the V–22 tiltrotor has been performed, to assess the validity of the formulation and to exploit the unique features of multi-body analysis with respect to conventional comprehensive rotorcraft codes; These are the ability to model the exact kinematics of mechanical systems, and the possibility to simulate unusual maneuvers and unusual flight conditions, that are particular to the tiltrotor, e.g. the conversion maneuvre. A complete modal validation of the analytical model has been performed, to assess the ability to reproduce the correct dynamics of the system with a relatively coarse beam model of the semispan wing, pylon and rotor. Particular care has been used to model the kinematics of the gimbal joint, that characterizes the rotor hub, and of the control system, consisting in the entire swashplate mechanism. The kinematics of the fixed and the rotating plates have been modeled, with variable length control links used to input the controls, the rotating flexible links, the pitch horns and the pitch bearings. The investigations took advantage of concurring wind tunnel test runs, that were performed in August 1998, and allowed the acquisition of data specific to the multi-body analysis.

Introduction

Traditional analysis of rotorcraft is based on well established methods, usually implemented in dedicated analysis tools. Transfer Matrix, or Myklestad, and FEA are used to determine the structural properties of flexible blades, such as frequencies and mode shapes. Dedicated formu-

1. Corresponding Author,
via La Masa 34, 20158, Milano
Tel.: ++39(02)3933-2393
Fax: ++39(02)3933-2334
E-mail: *masarati@aero.polimi.it*

Presented at the American Helicopter Society 55th Annual Forum, Montreal, Canada, May 25–27, 1999.

lations are used to study the basic behavior of rotors in trimmed hover and forward flight conditions. Examples are PASTA [13], DYN4-DYN5 [18]. Usually these formulations rely on basic assumptions that simplify the problem, thus improving the efficiency of the analysis and reducing the computational cost. On the other hand, usually, only a limited set of problems, with little flexibility in the choice of the configuration, can be effectively handled. Comprehensive codes give an important rotorcraft analysis capability. For years they have been the best trade-off between both the generality of the formulation and of the range of application, and reasonable simplifications. A relatively detailed structural description is usually allowed; the degrees of freedom are successively condensated by modal reduction, and the reduced model is used for subsequent aeroelastic analyses, ranging from trimmed solutions to aeroelastic stability. Examples are CAMRAD [10], [11], UMARC [9]. In some cases, a sophisticated aerodynamic analysis is used to determine the wake of the rotor, as in CAMRAD, UMARC, CAMRAD II [12]. A general purpose modeling code represents an analysis tool allowing the handling of a wide spectrum of problems with as little limitations as possible; the multi-body interdisciplinar approach is a clear example. A multi-body model has unique features with respect to more conventional approaches: there are no kinematic assumptions or simplifications. The kinematic behavior of a mechanism can be modeled to the desired degree of refinement, with exact kinematic relationships between bodies; elastic bodies can be modeled with a degree of refinement comparable to that of a nonlinear FEA; the designer is left a complete freedom on the description of the system, which is built from scratch component by component. This approach is likely to need more computer power than that required by specialized and simplified approaches, but pays back in terms of efficiency since it allows the designer to avoid risky physical oversimplifications along with the greater modeling confidence allowed by using a single, general purpose, and well proven modeling tool. Moreover, with the computer power nowadays available, even the most complex models are likely to require a turnaround time that is compatible with an extensive set of parametric analyses and, in a short time, even with a complete system optimization. The technology of multi-body is not mature yet, with particular regard to the aeronautical and specifically the aeroservoelastic field. Current commercial general purpose multi-body analysis codes, e.g. DADS [8], MECANO [3], ADAMS and others [20], still pose some limitations to the modeling of rotorcrafts, mainly due to insufficient aerodynamics, insufficient description of flexible bodies, and in some cases to limitations in the integration algorithms when applied to large finite rotations of the order of some revolutions [14]. A special case is represented by CAMRAD II, which should be considered something more than a comprehensive code, but not yet a general purpose, global modeling multi-body code. In the research field, a promising multi-body code, successfully applied in rotorcraft analyses, is DYMORE [1]. A brief description of the multi-body formulation applied in this paper is presented first, followed by a description of the tiltrotor model form a multi-body standpoint. Finally, the results of the analysis are discussed.

Multi-Body Formulation

Dynamics. The multi-body problem is formulated by directly writing the equilibrium equations of each body. Constraints are imposed by adding constraint equations, resulting in unknown "reacting forces" as unknowns, in a *Lagrangian Multipliers* style. The reaction unkowns are directly the reaction forces; this overcomes the need of post processing the multipliers to determine the reactions. The dynamics problem has been written as a first order differential system of equations; the equilibrium equations of a body are:

$$\begin{cases} \dot{\beta} - F\left(x, \dot{x}, R, \omega, t\right) = 0 \\ \dot{\gamma} - \left(\omega \times S\right) \times \dot{x} - M\left(x, \dot{x}, R, \omega, t\right) = 0 \end{cases}$$

where β, γ are the momenta, x is the position of the node, R is the rotation matrix that describes the rigid rotation from the local to the global frame, expressed in terms of the *Gibbs-Rodriguez* rotation parameters g, ω is the angular velocity of the node, related to the rotation matrix by $\omega\times = \dot{R}R^T$ where operator $\times$ represents the cross product; ω is related to the derivatives of the parameters by the expression $\omega = G\dot{g}$. The inertial forces and moments balance in a *d'Alembert* sense the forces F and moments M, which may depend on the configuration, e.g. the elastic forces, as well as on other parameters, like the time t. The term $(\omega \times S)\times\dot{x}$

in the moment equation is due to the motion of the pole the moments are referred to. The definitions of the momenta are:

$$\begin{cases} \beta = m\dot{x} - S \times \omega \\ \gamma = S \times \dot{x} + J\omega \end{cases}$$

The mass of the body is m; the inertial properties S, J represent the first and second order inertia moments of the body, referred to the global frame; their transformation from the local to the global frame is $S = R\tilde{S}$, $J = R\tilde{J}R^T$. Kinematic constraints are added as constraint equations:

$$\Phi\left(x, \dot{x}, R, \omega, \ldots, t\right) = 0$$

The unknown constraint reactions V_F, V_M contribute to the equilibrium equations as Lagrange multipliers. Equations Φ may represent holonomic (algebraic) and non-holonomic (differential) constraints. The resulting system of equations, made of the equilibrium equations, the definitions of the momenta and the constraint equations, is known as *Lagrangian* of the first kind, and it is Differential Algebraic (DAE) of index three [2]. The system is solved in the unknowns x, g, β, γ, V_F, V_M without any further substitution. Control and Servosystem equations are added as generic differential equations, with generic scalar unknowns. they are implemented in the so called *General elements*, or GENEL.

Kinematics. The formulation of the kinematics of finite rotations is fundamental in a multibody implementation. The orientation of a local frame is described by an orthogonal matrix R that maps vectors from the local to the global frame. The parametrization of large rigid rotations requires at least three unknowns, but four parameters are needed to avoid singularities that arise when the orientation of the rotation is undefined. This problem has been prevented by considering incremental unknown rotations. The current orientation of the generic reference frame R is accounted for by a constant rotation matrix R_r, multiplied by the unknown incremental rotation represented by matrix R_Δ, assumed to be small enough to avoid any singularity. This assumpion is reasonable since a limited rotation at each step is required for accuracy considerations. Matrix R_r is updated at each step. The Gibbs-Rodriguez parameters $g = 2\,\tan^{-1}\left(\varphi/2\right)$ represent a very efficient finite rotations parametrization from a computational standpoint, since they are entirely algebraic. The linearized expressions of the rotational entities concide with those of the rotational vector φ. The rotation matrix R is:

$$R = I + \frac{4}{4 + g^T g}\left(g \times + \frac{1}{2} g \times g \times\right)$$

while matrix G is:

$$G = \frac{4}{4 + g^T g}\left(I + \frac{1}{2} g \times\right)$$

Integrator. Time integration is performed by an implicit, A/L-stable, second order accurate predictor-corrector integrator. The basic formulas are:

$$\begin{aligned} \dot{y}_k &= -\frac{12}{h}\left(y_{k-1} - y_{k-2}\right) + 8\dot{y}_{k-1} + 5\dot{y}_{k-2} \\ y_k &= \left(1-\alpha\right) y_{k-1} + \alpha y_{k-2} + h\left(\delta + \frac{1}{2}\right)\dot{y}_k \\ &\quad + h\left(\frac{1}{2}\alpha + \frac{1}{2} - 2\delta\right)\dot{y}_{k-1} + h\left(\frac{1}{2}\alpha + \delta\right)\dot{y}_{k-2} \end{aligned}$$

for the predictor, consisting in the cubic extrapolation of the derivatives based on the states and their derivatives at the two preceding steps, and the prediction of the state based on an extrapolation, whose coefficients ensure second order accuracy, with user-defined control of the algorithmic damping; h is the time step. The formulas have been generalized to a variable step predictor. The coefficients α and δ can be expressed in terms of the desired asymptotic spectral radius ρ_∞, under the assumption of real and coincident asymptotic roots:

$$\alpha = \frac{4\rho_\infty^2 - \left(1-\rho_\infty\right)^2}{4 - \left(1-\rho_\infty\right)^2} \quad \delta = \frac{\left(1-\rho_\infty\right)^2}{2\left(4 - \left(1-\rho_\infty\right)^2\right)}$$

For $\rho_\infty = 1$ the method is very similar to the Crank-Nicholson rule (no dissipation), though using two steps, while for $\rho_\infty = 0$ the method coincides with the well known Backward Difference Formulas (BDF) [2]. The correction is performed by a complete/modified Newton-Raphson iteration.

Rotations Updating. The predicted configuration of the system is used as reference for the correction in a way called *updated-updated*. Only the rotation related to the correction is unknown; as a consequence, it is expected to be

really small, provided the prediction is accurate. The angular velocity becomes:

$$\omega = G_\Delta \dot{g}_\Delta + R_\Delta \omega_r$$

where subscripts $(\cdot)_\Delta$ underline that the rotation parameters and their derivatives are referred only to the correction rotation. As a consequence, when the prediction is accurate, the terms involved in the linearisations can be approximated as: $R_\Delta \cong I$, $G_\Delta \cong I$, $\omega \cong \dot{g}_\Delta + \omega_r$. The linearisations become:

$$\Delta R \cong \Delta g_\Delta \times R_r \qquad \Delta G_\Delta \cong 0$$

$$\Delta\omega \cong \Delta\dot{g}_\Delta + \Delta g_\Delta \times \omega_r$$

This greatly simplifies the writing of the Jacobian matrix, with consequent savings in computational time; the accuracy is preserved by consistently calculating the residual.

Beams. Beams are the main elastic element of the presented formulation. The strains are defined as the difference between the current and the initial derivatives of the reference line $p(\xi)$ that describes the position of the beam. The strains, in the material frame, are:

$$\tilde{\varepsilon} = R^T p' - \tilde{p}_0'$$

where the position p refers to the current frame, while $\tilde{p}_0$ refers to the initial configuration of the beam in the material frame, and the prime $(\cdot)'$ performs a spatial derivative with respect to an abscissa ξ along the reference line. The geometric curvature $\tilde{\rho}$ is defined as the spatial derivative of the reference frame of the beam section:

$$\tilde{\rho}\times = R^T R'$$

The difference between the current and the initial, or imposed, curvature $\tilde{\rho}_0$, represents the elastic curvature $\tilde{\kappa}$, again in the material frame:

$$\tilde{\kappa}\times = R^T R' - R_0^T R_0' = \tilde{\rho} \times -\tilde{\rho}_0\times$$

When incremental rotations are considered, the elastic curvature becomes:

$$\tilde{\kappa} = R^T G g' + \tilde{\kappa}_r$$

The above mentioned simplifications descending from the updated-updated rotations approach also apply to the beam kinematics. An original finite volume approach is used to formulate the beam element. Finite volumes applied to the equilibrium of a beam can be physically interpreted as the direct balance of the forces and the moments that act on a finite piece of beam, including the internal forces and moments at the boundary:

$$(I - U_b)\,\vartheta_b - (I - U_a)\,\vartheta_a = \mathcal{F}_a^b$$

where a and b label the ends of the piece of beam, $\mathcal{F}_a^b$ are the resulting dead forces and moments applied in the interval $[a, b]$, and matrix U represents the arm of the internal forces in the equilibrium equation of the moments:

$$U(\xi) = \begin{bmatrix} 0 & 0 \\ -(p(\xi) - x)\times & 0 \end{bmatrix}$$

being x the pole the moments are referred to. The internal forces are defined by means of a constitutive law in terms of the generalized strains, i.e. $\vartheta = \vartheta(\psi)$ where $\vartheta = \{\eta, \mu\}$ are the internal forces and moments and $\psi = \{\varepsilon, \kappa\}$ are the strains and the curvatures. An arbitrary, complete beam section characterization can be used, that fully couples the deformations and the forces, thus allowing the modeling of anisotropic beams [6], [4]. A three node parabolic C^0 beam element, that gives the exact solution for end-applied loads, has been implemented [15], [5]. The strains and curvatures at the boundaries of the finite piece of beam are expressed as functions of the nodal configuration by means of shape functions, thus resulting in a finite element-like discrete beam. The finite volume beam can be regarded as a constraint that relates the reaction forces to the deformation of the link, and thus to the configuration of the system. Provided the relation between reactions and configuration is invertible (i.e. the Hessian of the strain energy is positive definite), the constraint equation can be implicitly solved, thus allowing the direct writing of the contribution of the beam to the equilibrium equations in terms of position and rotation unknowns. Finite volume beams are easy to implement in a multi-body formulation since only collocated evaluation of the contributions to the equilibrium equations is required. Moreover, they straightforwardly resemble the natural partition in distinct bodies that is peculiar to the multi-body formulation. The finite volume description of the deformation of slender bodies is consistent with the mathematical, intrinsically discrete, multi-body model, and thus allows an easy but thorough

modeling.

Aerodynamic Forces. The aerodynamic forces are based on the strip theory, using elements that refer to rigid or beam shaped aerodynamic surfaces. The aerodynamic coefficients are based on the interpolation of experimental data spanning 360 degrees of angle of attack. Corrections are made to determine the drag due to spanwise flow, as well as the effects of dynamic stall [7]. Rotor elements are defined, to account for the effect of rotor induced velocity with an increasing degree of refinement, from uniform up to dynamic inflow modeling [17]. The implemented aerodynamic model is relatively poor, but it is satisfactory at least with regard to stability analysis. The code is being interfaced to a wake analysis program for more accurate airloads prediction.

Tiltrotor Models

The WRATS wind tunnel model is a semispan, 1/5 scale aeroelastic model of the V-22 tiltrotor [19]. It includes the right-side rotor, the pylon, and the half-wing. The rotor is powered by a water-cooled electric engine; the controls are applied to the swashplate by means of three hydraulic actuators. The basic geometric and structural properties have been taken from Ref. [16], from the drawings and from direct measures on the wind tunnel model. Each subpart of the tiltrotor has been modeled and analysed in its basic kinematic and dynamic features, then the parts have been assembled together and the complete system has been analysed. By using the same code and the same modeling for the single parts and the assembly, and by using a rather general approach in the kinematic and mechanical description of the single parts, any undue approximation has been avoided. The complete model is sketched in Figure 1.

Submodels

Blade. The single blade model has been used to analyse the dynamic properties of the blade, such as frequencies and aerodynamic properties. The flexbeam is described by a three-node beam element; a flexible control link is attached to the root of the blade by a rigid cuff and a pitch horn. The blade is joined to the outer end of the flexbeam by a spherical hinge, and by a spanwise oriented in-line joint, 2.2 in. outwards from the rotor axis. These bearings allow the free pitching of the blade; the flap and lead-lag motions result from the bending the flexbeam, simply supported by the bearings. A rigid blade has been used for preliminary evaluation of the kinematics of the rotor; most of the analyses has been performed with a flexible blade model. Two discretisations have been used, made of two and four beam elements respectively. The flexibility of the flexbeam and the position of the joints heavily affect the stability of the blade. The flapping is dominated by the gimbal, whose motion determines a negative δ_3 angle of about 15° (the pitch link is behind the blade). This is required to ensure the stability of the blade, being the rotor stiff-in-plane. But the virtual flap hinge due to the bending of the flexbeam is slightly outwards from the pitch link attachment, thus introducing a slight destabilizing effect on the flapping of the blade, which may become significant at high forward speeds, when the rotor acts as a propeller and the collective pitch at 75% of the blade is greater than 50°, because the flap and lag frequencies are very close to each other. This problem required a detailed study of the stiffness properties of the flexbeam.

Gimbal. The hub is attached to the mast by a gimbal joint. This joint allows the hub to flap freely about an arbitrary axis normal to the mast, while the torque about the shaft axis is transmitted. The gimbal mechanism is made of two universal joints, respectively linked to the mast and to the hub at one arm of each cross. The other arms of the two crosses are connected

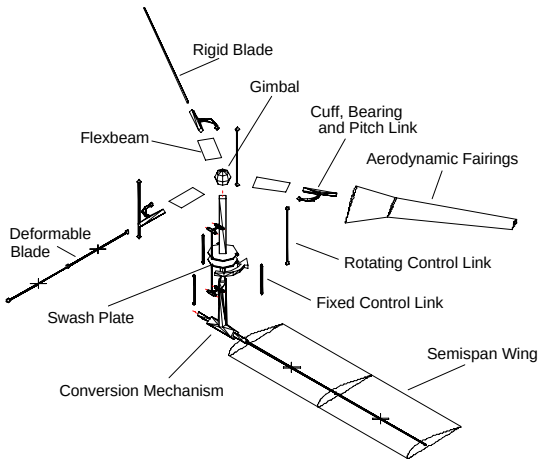

Figure 1: *Analytical Model*

to each other by a linkage, that transmits the torque between the mast and the hub and keeps the two universal joints at a constant distance. An in-line joint connects the hub to a spherical joint on the mast that represents the center of rotation of the hub. The gimbal is a complex joint that only in a very first approximation can be described by a simple universal joint. The multi-body approach easily allowed to model the complete kinematics of the joint from the beginning, thus ensuring the correctness of the formulation and with little computational overhead. The gimbal allows the rigid flapping of the whole rotor and, since the direction of the angular velocity tilts together with the hub, no Coriolis forces due to this motion result in the blades when the flapping is steady. At the same time, no stiffness due to centrifugal effects results from the 1 per rev. flapping motion, but that provided by a set of springs.

Swash Plate. The blade pitch is controlled by a swashplate. It has been modeled by two rigid bodies that represent the plates, linked together by a plane revolution joint. The fixed plate is forced to slide along an in-line joint with respect to the pylon; its position and attitude are controlled by three actuators. The controls are imposed by changing the length of the actuators. The two plates are respectively linked to the helicopter and to the shaft by scissors, that constrain the rotation about the shaft axis. The control links of the blades are attached to the rotating plate by simple pins. This allows the exact modeling of the kinematics of the pitch controls. Extensive analyses of the resulting pitch-flap and pitch-lag couplings have been performed, and good correlation with available data and with direct measurements on the model has been found.

Wing-Pylon. The wing model consists in two beam elements along the wing spar, at about 25% of the chord from the leading edge; the conversion hinge joint is at the wing tip, at about 75% of the chord, and it is elastically connected to the wing elements. The pylon is modeled as a rigid body. It is connected to the wing by the conversion joint, a flexible spindle that allows the free rotation about the conversion axis, while elastically constraining the bending in the other directions. The bending of the pylon about the axis normal to the wing is significant since it determines a coupled wing in-plane/pylon mode called the yaw mode, whose frequency is comparatively low [18]. The conversion is controlled by a conversion actuator located ahead of the hinge; this actuator at present is not mounted on the wind tunnel model, and a downstop spring is used to emulate its stiffness properties. Different sprins are used to change the conversion angle and to match the stiffness properties in the desired configuration. The analytical model has been tuned to reproduce these different stiffness configurations; the conversion actuator has been modeled, too, and conversion maneuvres have been simulated.

Results

The single submodels have been validated separately. Comparisons with experimental data and with results from previous analyses are presented. Partial assembly models of the rotor have been used for initial validations.

Blade Models. The very first analyses consisted in checking the kinematic couplings of the blade. Sample results are reported in Figure 2 where a comparison is made between the computed and the measured pitch-flap coupling. Subsequent analyses involved the identification of the frequencies and of the modes of the clamped blade. A very basic comparison was made with a corresponding NASTRAN model of the blade, sharing the same properties and the same discretisation used for the multi-body analysis, to assess the correctness of the formulation of the beam element. The results are summarized in Table 1

Rotor Models. The structural properties of the rotor have been analysed by means of many

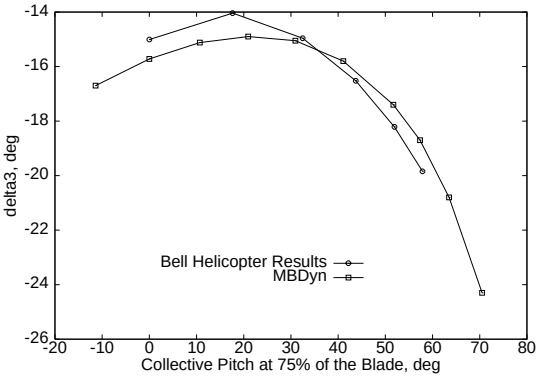

Figure 2: *Pitch-flap coupling*

Table 1: *Cantilevered blade frequencies, Hz*

MODE	GVT	UMARC	NASTRAN	MBDyn	
				4 el.	2 el.
1 B	12.29	12.3	11.5	11.3	11.7
1 C	34.11	34.1	33.4	33.1	32.7
2 B	52.44	53.0	56.7	55.8	55.0
1 T	113.35	111.4	127.0	119.0	122.0

different partial models. Basically, data from Ground Vibration Tests (GVT) of the non-rotating assembly, with clamped pylon and free or locked gimbal, as well as computed results from various sources were available. The single blade with the flexbeam and the locked control chain has been used to simulate the clamped gimbal condition. A complete model of the rotor has been used to simulate the free gimbal condition. It is important to notice that the three blade configuration and the gimbal joint break the symmetry of the system, thus requiring a modal analysis of the full rotor, being insufficient a simple superimposition of the clamped rotor modes to the flapping motion allowed by the gimbal. The results from the multi-body analysis of the complete three-blade rotor were later confirmed by modifying UMARC to allow the modeling of the full rotor in the modal analysis phase, as detailed later. Results are reported in Table 2

In vacuo rotating analyses have been compared only to numerical data since no experimental results were available. Myklestad and UMARC analysis results have been used. The full flight envelope has been tested, by performing modal analyses at the hover and forward flight rotation speeds and at different values of collective pitch. The change in pitch is significant when going from the hover condition to the forward flight at high speed, being of the order of 60°. Good agreement between all the available results has been found, as may be seen in Tables 3, 4. Data from Myklestad analysis refers to a clamped gimbal rotor, the missing values referring to non-symmetric modes that involve some gimbal flapping, as shown by multi-body and modified UMARC analyses.

Table 2: *Full rotor, non-rotating, Hz*

Mode	GVT	MBDyn	
	10 deg.	10 deg.	50 deg.
Gimbal	2.0	1.8	1.5
Cone	6.8	7.0	7.8
2 Flap	25.0	26.5	36.5
2 Flap asym.	64.2	57.1	55.0
3 Flap	76.2	78.0	82.5
1 Lag	19.7	19.0	12.7
2 Lag	91.3	98.0	92.0
1 Torsion	112.1	109.0	107.5

Table 3: *Rot. freq., 888 rpm,* $\theta_{75\%} = -3°$*, Hz*

Mode	Myklestad	UMARC	MBDyn
Gimbal	-	14.8	14.8
Cone	17.2	17.3	17.5
1 Lag	22.4	20.8	24.0
Coll Lag	42.	44.0	36.0
2 Flap	37.33	49.6	41.0
2 Flap a.	-	70.2	65.0
3 Flap	75.33	90.3	73.0
Flap/Tors.	89.33	92.7	90.0
Lag/Tors.	-	113.4	104.0
Torsion	-	116.0	110.0

Table 4: *Rot. freq., 742 rpm,* $\theta_{75\%} = 55°$*, Hz*

Mode	Myklestad	UMARC	MBDyn
Gimbal	-	12.4	12.6
Cone	14.7	14.9	15.1
1 Lag	15.3	15.8	16.5
2 Flap a.	-	42.3	44.2
Coll Lag	32.7	45.9	46.9
2 Flap	45.3	45.6	49.1
3 Flap a.	-	46.9	60.3
3 Flap	66.0	60.1	65.2
Flap/Tors.	89.3	90.6	97.8
Lag/Tors.	90.0	90.8	89.7
3 Lag	-	92.0	92.9
Torsion	-	116.0	108.5

Wing Model. A relatively coarse mesh has been used for the wing, so only the very first modes have been sought, by comparing to GVT and to NASTRAN [16] detailed analyses of the model, see Table 5. Particular care has been taken in modeling the downstop springs that are used to simulate the stiffness of the conversion actuator in the different configurations.

Wing-Rotor Models. The models of the wing and of the full rotor have been coupled to obtain the full detailed model of the tiltrotor. The complete model, with structural nodes, reaction unknowns and control-related unknowns has 580–600 degrees of freedom, depending on the type of analysis. A final check of the frequencies of the assembly has been made, followed by the aeroelastic analyses. The first wing modes are not

directly affected by the modeling of the flexibility of the rotor. The torsion mode of the wing is very close, and at some airstream speeds coincident, to the rotor speed; this gives raise to resonance that can be seen in the frequency analyses of the internal forces of the wing. Four wing modes are mainly considered: the beam, chord and torsion modes of the wing, and the previously mentioned pylon yaw mode. Referring to the fixed frame, the retreating rotor modes interact with the wing modes. This can be clearly appreciated from a frequency analysis of the wing response when the rotor modes are excited. Most of these modes cannot be easily identified when the aerodynamics are modeled, since they are highly damped. For this reason, a comprehensive analysis of the structural properties of the model has been performed by simulating *in vacuo* operations, while the aeroelastic properties have been estimated in different ways. The damping of the wing modes in forward flight has been estimated by system identification of the response to a given input, as is usually done during actual wind tunnel tests, while the aeroelastic pitch-flap coupling has been estimated by measuring the phase shift between an harmonic control input and the flapping response. Figure 3 refers to a collective pitch maneuvre. It shows the geometric pitch of one blade as the collective control is raised from 0 to 10 degrees in one second. The simulation is performed in helicopter mode; the nominal hover rotation speed of 888 rpm is reached in one second to obtain a trimmed condition (not shown); the residual oscillations at the beginning are due to the spin-up transient. There is no airstream speed. The difference between the given control and the actual pitch of the blade is due to the deformation of the flexbeam and of the flexible link. Figure 4 refers to the conversion maneuvre performed by a deformable blade model. It shows the internal forces at the wing root. The conversion is performed at a 10 deg/s constant angular speed. Oscillations of the internal forces due to the untrimmed initial conditions are appreciably damped as the maneuvre proceeds to the end, at $t = 9$ s. The following abrupt raise of the internal forces is due to the transient caused by the sharp end of the maneuvre. The flexible blade model has been used to simulate the response to a cosinusoidal vertical gust in airplane mode, of 10 ft/s amplitude. Both the stability and the sensitivity of the tiltrotor have been addressed. Figures 5, 6 show the wing out-of-plane internal moment due to the gust at different airstream speeds, for both off- and on-downstop configurations. In figure 5 the off-downstop configuration is clearly less damped than the other one, in fact the stability boundary in air is about 160 Kts. When the rotating speed is increased, the stability boundary moves towards lower speeds, as shown by previous analyses and experiments [18].

Table 5: *Wing frequencies, Hz*

Mode	d/s	GVT	NASTRAN	MBDyn
Beam	on	6.00	6.16	5.9
	off	5.51	5.45	5.4
Chord	on	8.45	9.33	9.1
	off	8.45	8.74	8.8
Torsion	on	12.5	12.6	12.5
	off	10.6	10.6	11.0
P. Yaw	on	16.5	18.9	17.2
	off	16.7	16.7	16.6

Computational Notes

The complete model has nearly 600 degrees of freedom. No modal condensation has been performed; the physical flexible elements have been used throughout the analyses. A typical model of the tiltrotor is made of 45 nodes, 39 rigid bodies, 35 joints of different kind, 18 beam elements, 14 aerodynamic elements, 6 control-related nodes and 4 control-related elements. The simulations have been performed on off-the-shelf PCs. The time step initially required for the rigid blade model was $\Delta t = .5 \times 10^{-3}$ s, while the deformable blade model required $\Delta t = .25 \times 10^{-3}$ s to start correctly. When a variable time step was used, the rigid blade model simulations quickly reached a value of

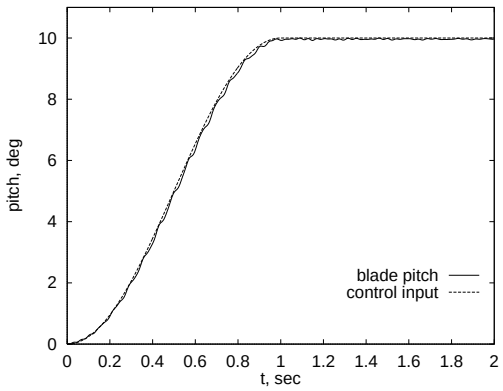

Figure 3: *Collective pitch maneuvre*

$3.0 \div 3.5 \times 10^{-3}$ s, while, the deformable blade model ones, reached about $1.0 \div 1.2 \times 10^{-3}$ s. The conversion simulation required about 4.5 hours on a Pentium PRO 200 for a total of 40000 fixed size time steps (10 s at $\Delta t = .25 \times 10^{-3}$ s). When performed with variable step size, it required about one hour. After the model was refined, and a soft start was used, the flexible blade model is able to start with $\Delta t = 10^{-3}$ s, requiring about 1.7 hours, or 1.1 hours on a Pentium II 333 and 0.8 hours on a Pentium II 450. Tests are being performed on Digital workstations with Alpha processor. The speed has been increased of a factor 4.5 for typical simulations. These numbers make this kind of analysis interesting even for a large, time consuming parametric study for rotorcraft design, not only for analysis.

Concluding Remarks

The paper illustrates the feasibility of a multibody, global modelling approach to the analysis of a rotorcraft. A tiltrotor has been chosen since its peculiarities are likely to highlight the possible limitations of more conventional analysis and design formulations when facing nonconventional configurations that may require the analysis of non-conventional flight conditions or maneuvres. The formulation proved to be efficient without excessive simplifications. The efficiency has been preserved while maintaining the physical meaning of both the equations and the unknowns. The multi-body formulation relies on the writing of the equilibrium equations of each body of the system, regarded as independent. Kinematic constraint equations are added, resulting in reaction unknowns that contribute to the equilibrium of the bodies. Finite, large rotations are accounted for in a computationally efficient way, based on an updated Lagrangian approach, that assumes the predicted configuration of a node as reference. The writing of the Jacobian matrix is simplified, resulting in computational time saving, while the accuracy is preserved by consistently computing the residual. A model of the tiltrotor used in WRATS investigation has been analysed, consisting in rotor models of increasing refinement, with rigid and flexible blades, the gimballed constant velocity joint, the swashplate and the control links, the pylon, the conversion hinge and the flexible wing. Aerodynamic loads have been considered, to simulate different test conditions, from aeroelastic stability investigations to the simulation of complex manoeuvers, including conversion and blade pitch control. The results here presented should be considered as an assessment of the validity of the formulation, rather than a complete analysis of the WRATS tiltrotor model. The multi-body code that resulted form the pro-

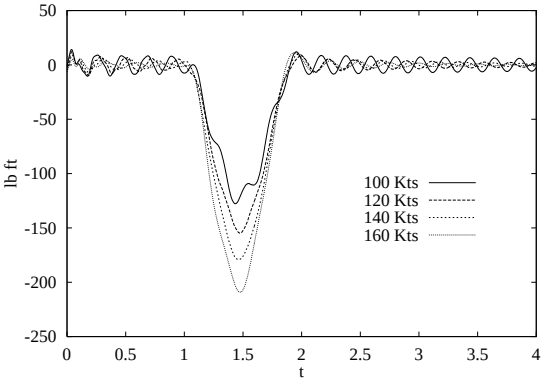

Figure 5: *Gust — off-downstop*

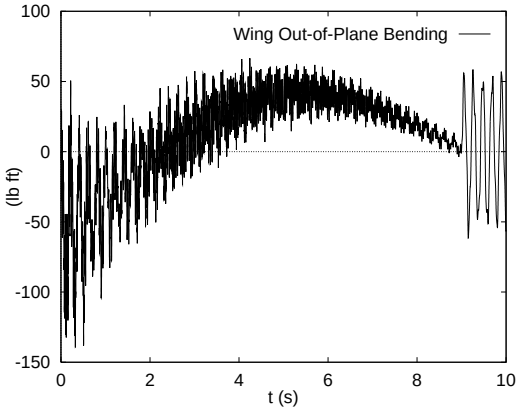

Figure 4: *Conversion — Bending moment*

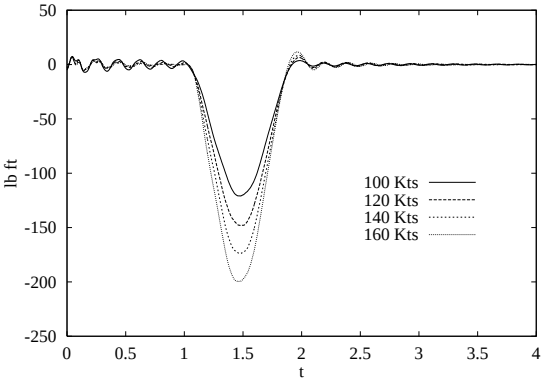

Figure 6: *Gust — on-downstop*

posed formulation is currently being improved by adding true active control capabilities, integrated electric and hydraulic networks analysis, modal description of flexible bodies, and, from a computational point of view, iterative, matrix-free solvers to speed-up the solution phase in view of a low-cost, coarse scale parallelization of the code.

Aknowledgments

The authors wish to aknowledge the NASA Langley Research Center and the Army Research Laboratory, which cooperated in providing data for the correlation studies.

References

[1] Bauchau, O. A., and N. K. Kang, "A Multibody Formulation for Helicopter Structural Dynamic Analysis", *Journal of the American Helicopter Society*, Vol. 38, N. 2, April 1986, pp. 3–14

[2] Brenan, K. E., S. L. Campbell and L. R. Petzold, "*Numerical Solution of Initial-Value Problems in Differential-Algebraic Equations*", North-Holland, New York, 1989

[3] Cardona A., "An Integrated Approach to Mechanism Analysis" Thèse de doctorat, Université de Liège, 1989

[4] Ghiringhelli, G. L. and P. Mantegazza, 1994, "Linear, Straight and Untwisted Anisotropic Beam Section Properties From Solid Finite Elements", *Composites Engineering* Vol. 4, N. 12

[5] Ghiringhelli, G. L., P. Masarati and P. Mantegazza, "A Multi-Body Implementation of Finite Volume Beams", accepted for publication by the *AIAA Journal*

[6] Giavotto, V., M. Borri, P. Mantegazza, G.L. Ghiringhelli, V. Caramaschi, G.C. Maffioli and F. Mussi, 1983, "Anisotropic Beam Theory and Applications", *Computer & Structures*, Vol. 16, No. 1–4

[7] Harris, F. D., Tarzanin, F. J. Jr., and Fisher, R. K. Jr., "Rotor High Speed Performance, Theory vs. Test", *Journal of the American Helicopter Society*, Vol. 15, No. 3, July, 1970, pp. 35–41

[8] Haug, E. J., *Computer Aided Kinematics and Dynamics of Mechanical Systems. Vol. 1: Basic Methods* Boston, Allyn and Bacon, 1989

[9] Hong, C. H., and Chopra, I., "Aeroelastic Stability Analysis of a Composite Rotor Blade", *Journal of the American Helicopter Society*, Vol. 30, No. 2, 1985, pp. 57–67

[10] Johnson, W., "Development of a Comprehensive Analysis for Rotorcraft — I. Rotor Model and Wake Analysis", *Vertica*, Vol. 5, 1981, pp. 99–129

[11] Johnson, W., "Development of a Comprehensive Analysis for Rotorcraft — II. Aircraft Model, Solution Procedure and Applications", *Vertica*, Vol. 5, 1981, pp. 185–216

[12] Johnson, W., "Technology Drivers in the Development of CAMRAD II", presented at the *American Helicopter Society Aeromechanics Specialists Conference*, San Francisco, California, January 19–21, 1994

[13] Kvaternik, R. G., "Studies in Tilt-Rotor VTOL Aircraft Aeroelasticity", Ph.D. Thesis, Case Western Reserve Univ., 1973

[14] Lanz, M., P. Mantegazza and P. Faure Ragani, "Aeroelastic Rotor Dynamics by General Finite Element and Multibody Approaches", *IX World Congress on the Theory of Machines and Mechanisms*, Vol. 2, pp. 1650–1656, August-September 1995, Milano, Italy

[15] Masarati, P. and P. Mantegazza, "On the C^0 Discretisation of Beams by Finite Elements and Finite Volumes", *l'Aerotecnica Missili e Spazio*, Vol. 75, pp. 77–86, 1997

[16] Parham, T. Jr., "A3B Semispan Model Stress Report", Bell Helicopter Internal Report No. 599-099-197, Nov. 11, 1994

[17] Pitt, M., and Peters, D. A., "Theoretical Prediction of Dynamic-Inflow Derivatives", *Vertica*, Vol. 5, 1981

[18] Popelka, D., M. Sheffler, J. Bilger, "Correlation of Test and Analysis for the 1/5-Scale V-22 Aeroelastic Model" *Journal of the American Helicopter Society*, Vol. 32, (2), Apr. 1987

[19] Settle, T. B., and D. L. Kidd, "Evolution and Test History of the V-22 0.2-Scale Aeroelastic Model", *Journal of the American Helicopter Society*, Vol. 37, (1), Jan. 1992

[20] Schiehlen, W., "Multibody Systems Handbook", Berlin Springer-Verlag, 1990